

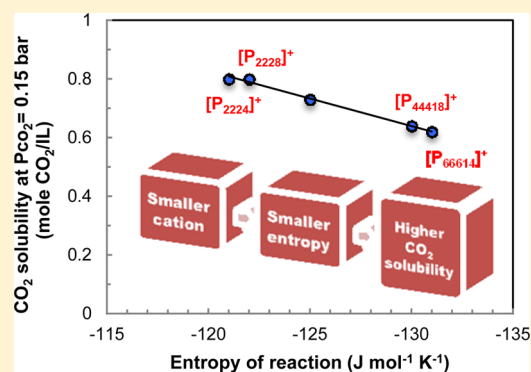
Effect of Cation on Physical Properties and CO₂ Solubility for Phosphonium-Based Ionic Liquids with 2-Cyanopyrrolide Anions

Samuel Seo, M. Aruni DeSilva, Han Xia, and Joan F. Brennecke*

Department of Chemical and Biomolecular Engineering, University of Notre Dame, Notre Dame, Indiana 46556, United States

S Supporting Information

ABSTRACT: A series of tetraalkylphosphonium 2-cyanopyrrolide ($[P_{nmmn}][2\text{-CNPyr}]$) ionic liquids (ILs) were prepared to investigate the effect of cation size on physical properties and CO₂ solubility. Each IL was synthesized in our laboratory and characterized by NMR spectroscopy. Their physical properties, including density, viscosity, and ionic conductivity, were determined as a function of temperature and fit to empirical equations. The density gradually increased with decreasing cation size, while the viscosity decreased noticeably. In addition, the $[P_{nmmn}][2\text{-CNPyr}]$ ILs with large cations exhibited relatively low degrees of ionicity based on analysis of the Walden plots. This implies the presence of extensive ion pairing or formation of aggregates resulting from van der Waals interactions between the long hydrocarbon substituents. The CO₂ solubility in each IL was measured at 22 °C using a volumetric method. While the anion is typically known to be predominantly responsible for the CO₂ capture reaction, the $[P_{nmmn}][2\text{-CNPyr}]$ ILs with shorter alkyl chains on the cations exhibited slightly stronger CO₂ binding ability than the ILs with longer alkyl chains. We attribute this to the difference in entropy of reaction, as well as the variation in the relative degree of ionicity.



INTRODUCTION

Ionic liquids (ILs) are defined as salts with melting points below 100 °C. The unusual properties of ILs, including extremely low vapor pressures, high thermal stabilities, and wide liquid ranges, make them excellent replacements for the current aqueous amine solutions used in postcombustion CO₂ capture from flue gas.¹ In addition to such physical properties, wide tunability allows one to tune the structure of the component ions. For instance, by tethering an amine functionality to the anion,^{2–6} cation,⁷ or both,⁸ ILs can be designed to react chemically with CO₂ even at low partial pressures. Unfortunately, most of these task-specific ILs suffer from high viscosity and slow kinetics for CO₂ capture, especially when they react with CO₂.⁹ Recently, our group proposed the use of aprotic heterocyclic anions (AHAs), which can react reversibly and in a 1:1 stoichiometric ratio with CO₂ with readily tunable enthalpy of reaction.^{4,10} Unlike other ILs that react with CO₂, the viscosity of these AHA ILs with tetraalkylphosphonium cations remain unchanged upon reaction with CO₂.¹¹

ILs with phosphonium cations are generally known for their high thermal stability^{12–14} and ease of large-scale production.¹⁵ In this context, ILs with a phosphonium cation are great candidates for absorbents used in postcombustion CO₂ capture processes. Especially, trihexyl(tetradecyl)phosphonium ($[P_{66614}]^+$) is one of the most commonly adopted cations in the development of ILs for CO₂ capture applications, as its bulkiness and asymmetry generally induce very low melting

points or glass transition temperatures regardless of the anion with which it is paired. However, its large molecular weight is disadvantageous in terms of volumetric and gravimetric CO₂ uptake ratio. Utilizing the tetraalkylphosphonium cation allows one to easily tune the size of the cation (and IL) by adjusting the length of the hydrocarbon substituents. In this regard, our group recently showed that phase-change ionic liquids (PCILs) can be used for postcombustion CO₂ capture. PCILs are ILs that turn from solid to liquid upon reaction with CO₂,¹⁶ and take advantage of IL tunability: shortening the hydrocarbon substituents on the tetraalkylphosphonium cation effectively increases the melting point, which is a key physical parameter that made the PCIL process thermodynamically feasible.¹⁷ In this study, a series of tetraalkylphosphonium ($[P_{nmmn}]^+$, n = number of carbons in each hydrocarbon substituent, where the n values do not have to be equal) ILs were synthesized and characterized to investigate the effect of cation size (by adjusting the alkyl chain length) on physicochemical properties such as viscosity, density, ionic conductivity, and CO₂ solubility. Each cation is paired with a 2-cyanopyrrolide anion, $[2\text{-CNPyr}]^-$: this anion was chosen based on its high CO₂ capacity, moderate enthalpy of reaction ($\Delta H_{\text{rxn}}^\circ$) with CO₂, excellent thermal stability,¹⁰ as well as fast CO₂-reaction kinetics.¹⁸ Owing to these favorable properties, Brown et al.¹⁹

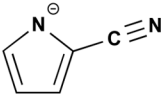
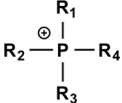
Received: June 16, 2015

Revised: August 3, 2015

Published: August 12, 2015



Table 1. Chemical Structures and Nomenclatures of $[P_{nnnn}][2\text{-CNPyr}]$ ILs

chemical structure	abbreviation	nomenclature
	$[2\text{-CNPyr}]^-$	2-cyano-pyrrolide
	$[P_{nnnn}]^+$	Tetraalkylphosphonium ^a

^a $[P_{2222}]^+$ = tetraethylphosphonium, $[P_{2224}]^+$ = triethyl(butyl)phosphonium, $[P_{2228}]^+$ = triethyl(octyl)phosphonium, $[P_{22212}]^+$ = triethyl(dodecyl)phosphonium, $[P_{44412}]^+$ = tributyl(dodecyl)phosphonium, $[P_{44418}]^+$ = tributyl(octadecyl)phosphonium, $[P_{66614}]^+$ = trihexyl(tetradecyl)phosphonium).

recently reported enhanced gravimetric CO_2 capacity and viscosity with $[2\text{-CNPyr}]^-$ with different cations, namely tetraalkylammonium and tetraalkylphosphonium, and their physical property trends and limited CO_2 uptake data are consistent with the more comprehensive results and analysis presented in this study.

Since ILs are composed entirely of ions, the IL system may be envisioned as a pool of free-flowing ions that are rapidly associating and dissociating. However, most ILs do not follow this ideal behavior due to strong interactions between two or more ions, and this may lead to formation of ion pairs or ion aggregations.²⁰ Recent molecular simulation work done by Yee et al. concluded that ILs do not behave like conventional alkali halide salts, and the ions of ILs can remain associated in aqueous solutions, even under highly diluted conditions.²¹ In this regard, ion pairs or aggregates, if sufficiently long-lived, can appear neutral, and thus they are not able to contribute to conduction.²² The degree to which ions are freely moving, as opposed to existing as ion pairs or aggregates, is frequently referred to as the “ionicity.” While Coulombic interactions are predominant in ILs, the van der Waals interactions must not be ignored, particularly when the cations include large hydrocarbons (e.g., $[P_{66614}]^+$). Therefore, in this study, we explore the relationship between the relative ionicity and the size of the IL (or cation). A Walden plot ($\log[\text{molar conductivity}]$ vs $\log[\text{viscosity}^{-1}]$) approach, as suggested by Angell and co-workers,²⁰ is one way of qualitatively assessing the ionicity. ILs with lower ionicity will exhibit substantially lower ionic conductivity than other ILs with similar viscosities, and this approach allows us to speculate on the relative ion conduction behavior in the $[P_{nnnn}][2\text{-CNPyr}]$ ILs in this study.

We also examine the effect of cation size on CO_2 solubility. Since Gurkan et al.² first reported the equimolar CO_2 uptake using anion-functionalized ILs under ambient conditions, the majority of our research efforts and those of others who have adopted the idea of functionalizing the anion to react with CO_2 have focused on tuning and modifying the anion moiety. While the choice of cation should be predominantly responsible for the physical properties of these ILs, the role of cation in CO_2 capture has been often neglected. On the other hand, Xu et al.²³ and Hollóczy et al.²⁴ reported that the basicity of ILs can be remarkably affected by the choice of the cation, as the degree of cation–anion interactions can enhance or reduce the basicity of the functionalized ion. It should be noted that several researchers have shown that a dialkylimidazolium cation (which is often considered inert when paired with a nonreacting anion) even has the potential to react with a CO_2 molecule via deprotonation of the acidic C(2) hydrogen

on imidazolium to form imidazolium-2-carboxylate when the cation is paired with a fairly basic anion (e.g., acetate or AHA).^{25–30} Recently, Gohndrone et al. discovered that the AHAs (and possibly other anions with similar basicities) are also capable of abstracting an acidic α -hydrogen atom of phosphonium cations to produce an ylide in the presence of CO_2 at elevated temperature.³¹ In this study, we show that somewhat different CO_2 uptake behavior was observed for a series of $[P_{nnnn}][2\text{-CNPyr}]$ ILs, and we attribute this to changes in the entropy of the reaction ($\Delta S_{\text{rxn}}^\circ$) of the anion with CO_2 caused by the cation.

MATERIALS AND METHODS

Chemicals and Synthesis. All ILs discussed in this study consist of the 2-cyanopyrrolide anion paired with various tetraalkylphosphonium cations. The chemical structure of each ion is shown in Table 1. Trihexyl(tetradecyl)phosphonium 2-cyanopyrrolide ($[P_{66614}][2\text{-CNPyr}]$) was prepared by a two-step synthesis protocol described in our previous work.⁴ First, SBR LG NC(OH) ion-exchange resin or Amberlite IRN78 (Sigma-Aldrich) in methanol (ACS grade, Fischer Scientific) was used to produce trihexyl(tetradecyl)phosphonium hydroxide ($[P_{66614}][\text{OH}]$) from trihexyl(tetradecyl)phosphonium bromide ($[P_{66614}][\text{Br}]$, 97% purity, Sigma-Aldrich). The resin was then washed with methanol three times at room temperature. After filtration of the resin, $[P_{66614}][\text{OH}]$ and the anion precursor, pyrrole-2-carbonitrile (98%, Alfa Aesar), were mixed in equimolar quantities, and an acid–base reaction produced the desired IL. The reaction lasted 12 h with stirring at room temperature. Excess methanol was separated by rotary evaporator at 50 °C.

For the preparation of ILs with tetraalkylphosphonium cations containing shorter alkyl substituents, a three-step procedure was adopted: the phosphonium halide precursor was prepared in the first step, followed by the anion exchange and acid–base neutralization (see Figure 1). Tributyl(C_n)-phosphonium bromide ($[P_{444n}][\text{Br}]$) and triethyl(C_n)-phosphonium bromide ($[P_{222n}][\text{Br}]$) were prepared via the alkylation of tributylphosphine (99%, VWR) or triethylphosphine (99%, Sigma-Aldrich), respectively. Corresponding trialkylphosphine and alkyl bromides, $C_n\text{H}_{2n+1}\text{Br}$ (>98%, Sigma-Aldrich) were reacted in acetonitrile and refluxed with stirring at 60 °C. 1-Iodooctadecane, $C_{18}\text{H}_{37}\text{I}$ (95%, Sigma-Aldrich), was used instead of the alkyl bromide for the preparation of tributyl(octadecyl)phosphonium iodide ($[P_{44418}][\text{I}]$). The alkylation step was performed under nitrogen atmosphere because of the sensitivity of the phosphine moiety toward oxygen in the air.³² Residual acetonitrile and

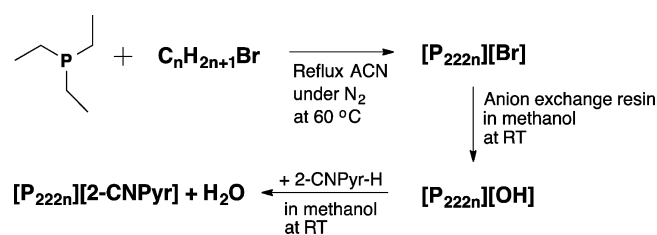


Figure 1. Schematic of $[P_{222n}][2\text{-CNPy}]$ synthesis procedure. The synthesis of $[P_{444n}][\text{AHA}]$ ILs was started via alkylation of tributylphosphine.

alkyl halide resulting from the alkylation step were removed by washing several times with hexane. The corresponding tetraalkylphosphonium hydroxide ($[P_{444n}][\text{OH}]$ or $[P_{222n}][\text{OH}]$) solutions were obtained by anion exchange, as described above. The tetraalkylphosphonium hydroxide solutions were then reacted with an equimolar amount of the heterocyclic precursor (pyrrole-2-carbonitrile) at room temperature to produce $[P_{444n}][2\text{-CNPy}]$ or $[P_{222n}][2\text{-CNPy}]$ along with water. All ILs were dried at 60 °C under reduced pressure for at least 48 h before use. A Brinkman 831 Karl Fischer coulometer was used to determine water content, and all samples contained lower than 1000 ppm water. ^1H NMR (Varian INOVA-500) and ^{31}P NMR (Varian INOVA-300) spectroscopy with deuterated DMSO- d_6 (99.9 atom % D, Sigma-Aldrich) as a solvent were used for IL analysis. Furthermore, bromide content was analyzed with a DIONEX DX-500 ion chromatograph was used to determine the bromide content, which was below 20 ppm in all cases. The purity of all ILs in this study is estimated to be greater than 98 mol % based on NMR spectroscopy. The ^1H NMR spectral assignments can be found in the [Supporting Information](#).

Characterization Methods. An oscillating U-tube densitometer (Anton Paar model DMA 4500) was used to measure the densities under ambient pressure. The temperature of the densitometer was controlled from 10 to 70 °C with a precision of ± 0.01 °C. Considering the purity of ILs (>98%), the uncertainty in the density measurements is approximately $\pm 1 \times 10^{-3}$ g cm^{-3} .

The viscosity measurements were carried out with an ATS Rheosystems Viscoanalyzer, which operates with a cone-and-plate spindle. To prevent the absorption of atmospheric moisture and CO_2 into the ILs, the sample chamber had nitrogen gas (Praxair grade 4.8, 99.998%, $\text{H}_2\text{O} < 3$ ppm) flowing over the sample throughout the measurements. The measurements were performed at controlled temperatures with

heating from 10 to 70 °C. The uncertainty is approximately $\pm 5\%$ above 100 cP and $\pm 10\%$ below 100 cP.

The ionic conductivity was determined by electrochemical impedance spectroscopy (EIS) (Solatron SI 1260 impedance/gain-phase analyzer and Solartron 1287 electrochemical interface). The cells were purchased from Materials Mates, and they consist of two Pt electrodes. Prior to the conductivity measurements, the cell constant for each cell was determined using diluted KCl standard solutions (from Palintest) as references. To minimize the exposure to atmospheric moisture and CO_2 , the IL samples were loaded into the conductivity cell in the nitrogen glovebox. The temperature was controlled from 10 up to 70 °C in a Binder refrigerated incubator KBS3 (E3.1). About an hour was allowed for the sample to reach the desired temperature prior to each measurement. The uncertainty in the conductivities is approximately $\pm 3\%$.

A Mettler-Toledo differential scanning calorimeter (DSC) (model DSC822e) was used to determine melting points (T_m) and glass transition temperatures (T_g). The samples were placed in a Mettler-Toledo standard 40 μL aluminum crucible with lid, and heated under N_2 from -120 to 110 °C at a heating rate of 10 °C min^{-1} . The onset point and midpoint were used to determine T_m and T_g , respectively. The uncertainties in the reported T_m and T_g values are approximately ± 1 °C.

The thermal stability of the ILs was determined with a thermal gravimetric analyzer (TGA) (Mettler Toledo TGA/SDTA 851e/SF/1100 °C). The nitrogen gas flow rate was controlled by a Gilmont Industries PMR1-010750 flowmeter at 50 mL min^{-1} . A 20 mg aliquot of sample in a 40 μL aluminum crucible (without lid) was heated at 10 °C min^{-1} , after being initially dried in situ at 110 °C for 45 min. The decomposition temperature (T_{dec}) in this study is the intersection of the baseline weight (after the drying step) and the tangent of the weight versus temperature curve once decomposition starts. The TGA has an accuracy of ± 0.25 °C; however, when one must manually identify the tangent point this increases the uncertainty to ± 2 °C. Both the TGA and the DSC use Mettler-Toledo STARe software 12.10.

CO_2 Solubility Measurements. The CO_2 solubility in each IL was measured at room temperature (22 °C) using a volumetric method with a custom-built instrument. The instrument consists of two main parts, a CO_2 reservoir and a reaction cell with known volumes (177 and 127 mL, respectively). The temperature in each system was determined using a type K thermocouple (Omega HH501DK, ± 0.5 °C uncertainty). The pressure in the reservoir and the reaction vessel was monitored with a model CM dial pressure gauge (± 2 mbar uncertainty) and a Heise model PM digital pressure

Table 2. Thermal Properties and Parameters for Density, Viscosity, and Conductivity Data

cation	thermal property			density		viscosity			conductivity		
	T_m	T_g	T_{dec}	a	b	η_0	α	T_g	σ_0	B	T_g
	K	K	K	g cm^{-3}	$10^{-4} \text{ g cm}^{-3} \text{ K}^{-1}$	cP	K	K	mS cm^{-1}	K	K
$[P_{2222}]^+$	282, 292	na ^a	576			0.389	593	195			
$[P_{2224}]^+$	312	193	578	1.151	-5.48	0.390	583	199	1397	777	180
$[P_{2228}]^+$	na ^a	196	567	1.122	-5.58	0.042	1110	167	802	812	181
$[P_{22212}]^+$	215, 233	na ^a	570	1.115	-5.67	0.065	1063	172	1331	1165	164
$[P_{44412}]^+$	na ^a	200	582	1.084	-5.68	0.185	897	181	154	743	197
$[P_{44418}]^+$	278	na ^a	588	1.075	-5.70	0.177	920	183	72	730	196
$[P_{66614}]^+$	na ^a	196	589	1.073	-5.78	0.180	904	175	60	741	196

^ana = a melting point or glass transition temperature does not exist for this IL.

indicator (± 0.5 mbar uncertainty), respectively. Approximately 2 g of pure IL sample was transferred to the reaction cell under a nitrogen environment. Then the reaction cell was evacuated using a vacuum pump (Welch Gem 8890), and CO_2 was fed from the reservoir into the reaction cell. The amount of CO_2 that entered the reaction cell was calculated based on the pressure drop in the reservoir. Upon the activation of the stir bar, the pressure of the reaction cell decreased rapidly, confirming the absorption of CO_2 gas into the IL. The temperature and pressure in the reaction cell were logged until the pressure no longer changed (vapor–liquid equilibrium). The CO_2 solubility in the IL at each pressure was determined from the total pressure drop using the ideal gas law with the Lee–Kesler correlation.³³ The uncertainty in the CO_2 solubility measurement is ± 0.02 mol CO_2/IL .

RESULTS AND DISCUSSION

Thermal Properties. The DSC results are listed in Table 2, along with the thermal stabilities of the $[\text{P}_{nmmn}][2\text{-CNPyrr}]$ ILs obtained from the TGA. No endothermic peak, corresponding to a melting point was observed for $[\text{P}_{2228}]^+$, $[\text{P}_{44412}]^+$, and $[\text{P}_{66614}]^+$ ILs in the cycle of the measurements. On the other hand, ILs with $[\text{P}_{2222}]^+$ or $[\text{P}_{2224}]^+$ cation showed distinct melting transition(s) around room temperature, due to a closer packing of the ions facilitated by small, symmetric cations. For the ILs that exhibited glass transition temperatures, the phase transition occurred in the range of -70 °C. The TGA results confirm that most of the $[\text{P}_{nmmn}][2\text{-CNPyrr}]$ ILs have excellent thermal stability around or above 300 °C at a scan rate of 10 °C min^{-1} . As previously reported by Brown et al.,¹⁹ the decomposition temperature, T_{dec} seems to be independent of the alkyl-chain length on the cation. We have previously shown that the thermal stability of the AHA-based ILs depends more strongly on the choice of the anion species (i.e., the basicity of the anion).⁴

Density. The densities of the $[\text{P}_{nmmn}][2\text{-CNPyrr}]$ ILs as a function of temperature are shown in Figure 2 and given in

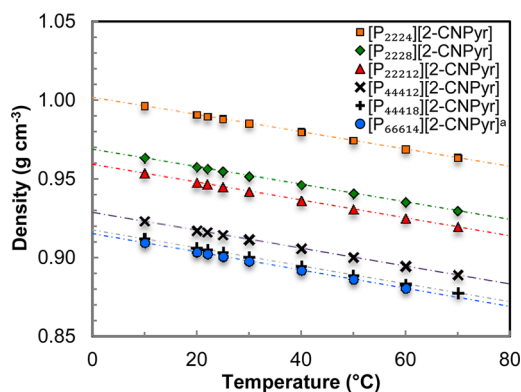


Figure 2. Density of $[\text{P}_{nmmn}][2\text{-CNPyrr}]$ as a function of temperature. (a) Values from Gurkan et al.¹⁰

tabular form in the Supporting Information. As observed in Figure 2, the densities decrease linearly with increasing temperature, and the best-fit parameters for the linear dependence of density with temperature ($\rho = a + bT$) are listed in Table 2. The density of $[\text{P}_{2222}][2\text{-CNPyrr}]$ was not measured, anticipating the solidification of the sample in the densitometer. All the $[\text{P}_{nmmn}][2\text{-CNPyrr}]$ ILs in this study had similar volume expansion with increasing temperature, as

indicated by the similar slopes of the linear fits. The densities of all ILs at room temperature are less than that of water, ranging in values from 0.903 to 0.990 g cm^{-3} for $[\text{P}_{66614}][2\text{-CNPyrr}]$ and $[\text{P}_{2224}][2\text{-CNPyrr}]$, respectively. The density increased with decreasing cation alkyl chain length ($[\text{P}_{66614}]^+ < [\text{P}_{44418}]^+ < [\text{P}_{44412}]^+ < [\text{P}_{22212}]^+ < [\text{P}_{2228}]^+ < [\text{P}_{2224}]^+$) without exception. This trend is consistent with previously studied imidazolium salts, in which an increase in the alkyl chain length on the imidazolium ring systematically reduced the density.^{34–38} Unlike trends observed for viscosity and conductivity, the density is rather insensitive to the symmetry of the cation, and is mainly dependent on the total number of carbons in the alkyl substituents.³⁹ The variation in the densities of the $[\text{P}_{nmmn}][2\text{-CNPyrr}]$ ILs is much larger than that of various $[\text{P}_{66614}][\text{AHA}]$ ILs from our previous paper,⁴ and this is primarily due to significantly larger variation in the free volume (and molecular weight) among different phosphonium cations in this study. The molar volume increased with increasing cation size, as shown in Figure S1 in the Supporting Information. In addition, the effective size of the ions were estimated by calculating van der Waals volumes, as well as by optimizing the ion structure using Density Functional Theory (DFT) calculations. From the comparison between the molar volume from the density (the total volume occupied by an IL system) and van der Waals/DFT volume (sum of volume occupied by each ion), it is clear that the ILs with larger cations have significantly greater free volume (see Table S5 and Figure S2 for details).

Viscosity. The temperature dependence of the viscosity for the seven 2-cyanopyrrolide ILs is presented in Figure 3 and

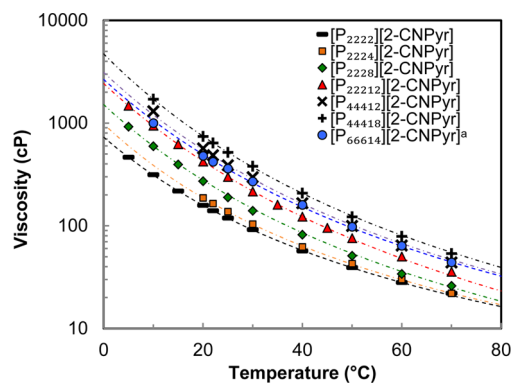


Figure 3. Viscosity of $[\text{P}_{nmmn}][2\text{-CNPyrr}]$ ILs as a function of temperature. (a) Values from Gurkan et al.¹⁰

given in tabular form in the Supporting Information. The two ILs with the shortest alkyl chains, $[\text{P}_{2222}][2\text{-CNPyrr}]$ and $[\text{P}_{2224}][2\text{-CNPyrr}]$, both have melting points near or slightly above room temperature, resulting from their highly symmetric cations; however, both remained subcooled liquids during the course of the viscosity measurements. The viscosity increased in the following order: $[\text{P}_{2222}]^+ < [\text{P}_{2224}]^+ < [\text{P}_{2228}]^+ < [\text{P}_{22212}]^+ < [\text{P}_{66614}]^+ \cong [\text{P}_{44412}]^+ < [\text{P}_{44418}]^+$. Such relationship between the length of the alkyl-chain and the viscosity is consistent with the trends exhibited by previously reported phosphonium-based,^{19,39} imidazolium-based³⁴ ILs, and alkyimidazoles.⁴⁰ It is apparent that the viscosity is strongly correlated with the length of the *n*-alkyl substituents on the cation: the viscosity of the $[\text{P}_{2222}]^+$ IL is five times lower than the $[\text{P}_{44418}]^+$ IL at room temperature. While the hydrogen-bond strength between 2-

CNPyr]⁻ and [P_{nnnn}]⁺ (between the nucleophilic site of the anion and the proton on the α -carbon of the cation) is expected to be similar for all of the ILs, the strength of van der Waals forces increases gradually with an elongation of the alkyl chains on the phosphonium cation, eventually increasing the friction and slowing down the dynamics of the ions. In addition, Tsunashima et al. attributed the decrease in viscosity upon shortening of the alkyl substituents to smaller Stokes radii of the cations.⁴¹ [P₄₄₄₁₈][2-CNPyr] has higher viscosity than [P₆₆₆₁₄][2-CNPyr] despite a slightly lower molecular weight (MW = 546.9 and 574.9 g mol⁻¹, respectively). The temperature dependency of viscosity may be described by a Vogel–Fulcher–Tammann (VFT) equation:⁴²

$$\eta = \eta_0 \exp\left(\frac{\alpha}{T - T_g}\right) \quad (1)$$

where η = viscosity in cP, T = absolute temperature, T_g = glass transition temperature in absolute units, and η_0 and α are adjustable parameters. In this study, T_g was used as an additional fitting parameter instead of applying experimentally measured values since several ILs lack T_g values. The dotted lines in Figure 3 represent the VFT model fit using the parameters summarized in Table 2.

Conductivity. The conductivities of [P_{nnnn}][2-CNPyr] ILs were measured from 10 to 70 °C, and the results are shown in Figure 4 and in tabular form in the Supporting Information.

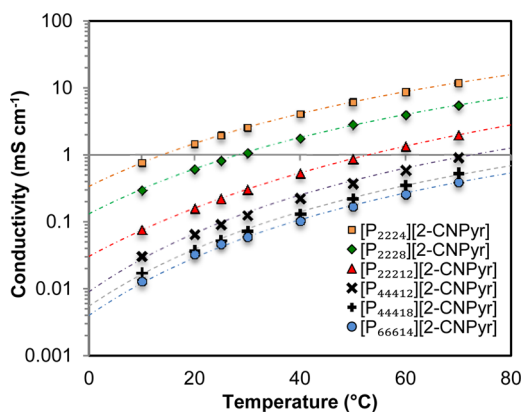


Figure 4. Conductivity of [P_{nnnn}][2-CNPyr] ILs as a function of temperature.

Ionic conductivities of the ILs are inversely proportional to their viscosities since ion mobility for conduction is predominantly restricted by the viscosity: the increasing order of ionic conductivity shown in Figure 4 is the reverse of the viscosity trend presented in Figure 3. The VFT equation was also used for modeling the conductivity data (η_0 and α in eq 1 are replaced by σ_0 [mS cm⁻¹] and $-B$ [K], respectively), and Table 2 shows the best-fit parameters.

Walden Plot. The interdependence of viscosity and ionic conductivity was analyzed using a Walden plot. A Walden plot emphasizes differences in conductivity of various ILs as a function of viscosity. Deviations from the “ideal” line, which runs from corner to corner and is constructed from data for dilute KCl aqueous solutions (generally considered to be fully dissociated ions), is a qualitative measure of the ionicity of an IL.^{20,22} The further an IL falls below this “ideal” line, the lower its ionicity. Unfortunately, the concept of “ionicity” tends to

create static images of anion/cation association/dissociation or aggregation. Obviously, ionic conductivity and viscosity are transport properties so they depend on the dynamics of the system. Thus, as mentioned in the Introduction, we interpret ionicity more in terms of how long-lived the association is between the cation and anion pair, or between aggregates of ILs.

As shown in Figure 5, all [P_{nnnn}][2-CNPyr] ILs fall below the ideal line as expected. While the Walden plot can only be used

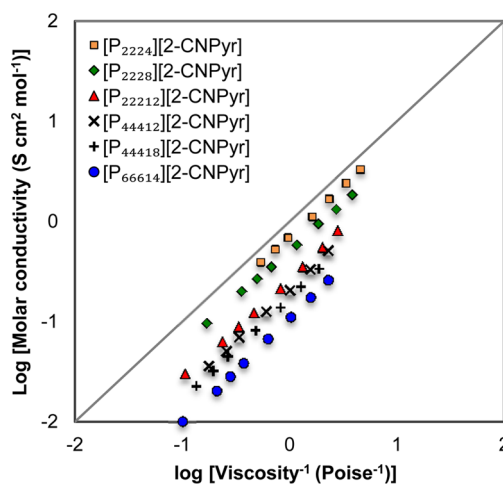
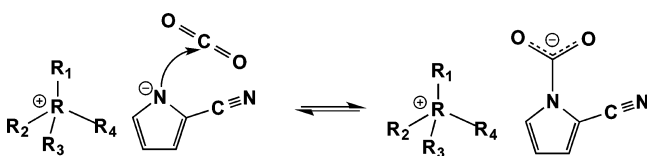


Figure 5. Walden plot of [P_{nnnn}][2-CNPyr] ILs.

as a qualitative tool for assessing relative ionicity, it is apparent that the distance from the ideal line increases systematically with increasing size of the phosphonium cation. ILs with smaller cations have lower viscosities, and they have relatively higher conductivities for these viscosities. On the other hand, for ILs with larger cations, the cations and anions must be less dissociated (i.e., have longer cation/anion contact times) as they exhibit lower conductivity for their particular viscosity range. Per the description given by Angell and co-workers,²⁰ [P₂₂₂₄][2-CNPyr] would be considered a relatively “good” IL, as opposed to [P₆₆₆₁₄][2-CNPyr] being a “poor” IL in comparison to the ILs with smaller cations. We believe this occurs primarily because a cation with longer hydrocarbon substituents experiences more extensive van der Waals interactions, leading to decreased mobility of the ions that predominantly governs the ionic conductivity. Similar trends have been observed for imidazolium bis-(trifluoromethanesulfonyl)amide⁴³ and tri-*n*-butylalkylphosphonium-based³⁵ ILs. Furthermore, an anion residing in close proximity to the center of a cation may be “trapped” by the long alkyl chains of neighboring phosphonium cations as hydrocarbons align easily with respect to one another and form aggregates or clusters to some extent.⁴⁴ Such extensive ion pairing or aggregation lowers an ion’s ability as a charge carrier, which may contribute to decreased ionic mobility and lower conductivities relative to their viscosities. In general, the slope of each line representing different ILs is approximately unity, indicating that the conductivity–fluidity relationship in all ILs remains roughly constant with increasing temperature. In an attempt to provide explicit allowance for differences in ion sizes, we also constructed an adjusted Walden plot (see Figure S3), as suggested by MacFarlane et al.²² While the relative distance between each IL appears to be slightly smaller after the size correction, the trend remains the same.

CO₂ Solubility. The CO₂ solubilities in ILs with functionalized anions are primarily dependent on the enthalpy of reaction ($\Delta H_{\text{rxn}}^{\circ}$ or the strength of anion–CO₂ interaction), between a reactive anion and a CO₂ molecule,⁴ and the contribution from the cation is often considered negligible. Our previous work has shown that the [2-CNPyr][−] anion is capable of reacting with CO₂ in an equimolar ratio,¹⁰ as depicted in Scheme 1.

Scheme 1. Complexation Mechanism of CO₂ with [P_{*n*}][2-CNPyr]



The CO₂ equilibrium isotherms for all of the ILs investigated here were obtained at room temperature; [P₂₂₂₂][2-CNPyr] solidified shortly after exposure to CO₂, and is not included in Figure 6. Since all ILs in this study have the same [2-CNPyr][−]

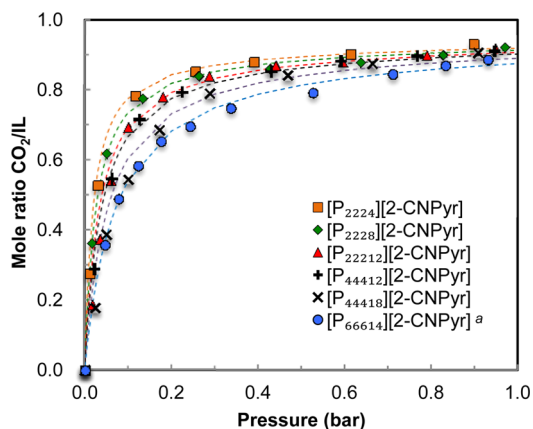


Figure 6. CO₂ solubility in [P_{*n*}][2-CNPyr] at 22 °C. (a) Values from Gurkan et al.¹⁰

anion, the CO₂ binding mechanism (see Scheme 1) and, therefore, the CO₂ solubility, are expected to be similar. As shown in Figure 6, however, the CO₂ solubility in [P_{*n*}][2-CNPyr] ILs varies with the variation in the *n*-alkyl substituents on the phosphonium cation: the smaller the cation is, the higher is the CO₂ solubility. Especially in terms of the gravimetric ratio of CO₂ uptake, the ILs with small cations have remarkably higher CO₂ solubility owing to their low molecular weight. At 0.15 bar (typical CO₂ partial pressure in postcombustion flue gas), the gravimetric CO₂ solubility increases from 1.08 to 3.00 mmol g^{−1} as the cation is changed from [P₆₆₆₁₄]⁺ to [P₂₂₂₄]⁺ (see Table 3). Note that if the physical dissolution of CO₂ was significant, which is not the case at these low partial pressures (see below), one would expect the solubility to be higher in the ILs with the longer chains.^{45–47}

The lines that go through the experimental data in Figure 6 are obtained using a Langmuir-type model (eq 2) described in our previous work:^{4,48}

Table 3. [P_{*n*}][2-CNPyr] Molecular Weight, CO₂ Solubility ($P_{\text{CO}_2} = 0.15$ bar), Equilibrium Constants, and Standard Entropy of Reaction at 22 °C

cation	molecular weight	CO ₂ solubility ($P_{\text{CO}_2} = 0.15$ bar)		K_{eq}^a	$\Delta S_{\text{rxn}}^{\circ b}$
	g mol ^{−1}	mole ratio mole CO ₂ per IL	gravimetric ratio mmol g ^{−1}		
[P ₂₂₂₄] ⁺	266.4	0.80	3.00	43.3	−121
[P ₂₂₂₈] ⁺	322.5	0.80	2.45	40.1	−122
[P ₂₂₂₁₂] ⁺	378.6	0.73	1.92	24.4	−124
[P ₄₄₄₁₂] ⁺	462.8	0.72	1.59	26.1	−125
[P ₄₄₄₁₈] ⁺	546.9	0.64	1.17	15.3	−129
[P ₆₆₆₁₄] ⁺	575.0	0.62	1.08	13.7	−131

^aHenry's constants and C_3 were fixed at 62 bar and 0.92, respectively.

^b $\Delta H_{\text{rxn}}^{\circ}$ was fixed at -45 kJ mol^{−1}.

$$z = \frac{P_{\text{CO}_2}/H}{1 - P_{\text{CO}_2}/H} + \frac{K_{\text{eq}} \cdot P_{\text{CO}_2} \cdot C_3}{1 + K_{\text{eq}} \cdot P_{\text{CO}_2}} \quad (2)$$

where Z is the molar ratio of CO₂ absorbed per IL, P_{CO_2} is the CO₂ pressure in bar, H is the Henry's law constant in bar, K_{eq} is the reaction equilibrium constant, and C_3 is the fraction of active IL (≈ 1). The Henry's law constant (H) is a measure of the physical solubility in ILs and is fixed at 62 bar, an experimentally measured value for [P₆₆₆₁₄][2-CNPyr] at 22 °C.^{10,44} While we would expect the Henry's law constants to be marginally higher (i.e., lower physical solubility) for the ILs with shorter alkyl chains on the cation because of reduced free volume, the physical solubility is so low at these low partial pressures of CO₂ that the value of the Henry's law constant does not noticeably affect the fit of the data. In fact, the physical solubility is expected to contribute only 1–2% of the total CO₂ uptake at 1 bar. C_3 has also been fixed at 0.92, as all the isotherms tend to level off around 0.92 mol CO₂/IL. Using the Levenberg–Marquardt method, the reaction equilibrium constant, K_{eq} , was then fit to the experimental CO₂ solubility data for each IL, and the resulting values are summarized in Table 3. The model fits the data very well for all of the ILs, as shown in Figure 6.

Since the $\Delta H_{\text{rxn}}^{\circ}$ between IL and CO₂ is primarily determined by the reaction between the anion and a CO₂ molecule, as depicted in Scheme 1, all ILs in this study should lend themselves to similar $\Delta H_{\text{rxn}}^{\circ}$ ($= -45$ kJ mol^{−1}, experimentally determined value reported by Gurkan et al.¹⁰). On the other hand, it is possible that the entropy of reaction ($\Delta S_{\text{rxn}}^{\circ}$) may vary for the different [P_{*n*}][2-CNPyr] ILs, mainly due to different degrees of reorganization that must take place for the anion to react with CO₂. We attribute this to the conformation of the cation, in terms of how it is associated with the anion and how long-lived that association may be. Using a general thermodynamic relation $\Delta G_{\text{rxn}}^{\circ} = -RT \ln(K_{\text{eq}}) = \Delta H_{\text{rxn}}^{\circ} - T\Delta S_{\text{rxn}}^{\circ}$, where R is gas constant, the parameter $\Delta S_{\text{rxn}}^{\circ}$ can be determined from known values of K_{eq} and $\Delta H_{\text{rxn}}^{\circ}$ (rearranging the above equation gives $\Delta S_{\text{rxn}}^{\circ} = R \ln(K_{\text{eq}}) + \Delta H_{\text{rxn}}^{\circ}/T$). In other words, $\Delta S_{\text{rxn}}^{\circ}$ can be regarded as a dependent variable that determines the equilibrium shift between the CO₂-binding reaction, assuming $\Delta H_{\text{rxn}}^{\circ}$ is constant for a given anion. As shown in Table 3, it is clear that the magnitude of $\Delta S_{\text{rxn}}^{\circ}$ increases (in absolute values) with increasing size of the cation. $\Delta S_{\text{rxn}}^{\circ}$ of -131 J mol^{−1} K^{−1} for [P₆₆₆₁₄][2-CNPyr] is in excellent agreement with the experimental value obtained from temper-

ature-dependent CO₂ solubility data.¹⁰ The increased magnitude of $\Delta S_{\text{rxn}}^{\circ}$ for larger cations might be interpreted as greater molecular reorientation during the CO₂ capture reaction, which eventually shifts the equilibrium toward the reactant side compared to the cases in which the cations (therefore, magnitude of $\Delta S_{\text{rxn}}^{\circ}$) are relatively smaller. The increasing free volume with increasing cation size, as described in Figure S2, also corroborates such argument.

Interpreting the CO₂ uptake curves in this way, it is clear that the standard entropy change for the reaction of the anion with CO₂ is related to the “ionicity” of the various [P_{*n*}][2-CNPy] ILs. As discussed in the previous section, the qualitative measure of ionicity for [P_{*n*}][2-CNPy] ILs from the Walden plot indicated that the ILs with smaller cations are less associated (i.e., shorter-lived interactions) compared to the ILs with larger cations. While the strength of the primary intermolecular interaction between the alpha hydrogen of the cation and the nucleophilic site of the anion should remain the same for all ILs in this study, the degree of relative ionicity (ion association/longevity of the interactions which could include IL aggregates) varies significantly with the extent of van der Waals interactions. ILs with relatively low ionicity are likely to have a reduced chance of reacting with a CO₂ molecule because of the presence of ion pairs or clusters. In addition, anions are attracted to positive charge density, which is positioned at the center of the phosphonium cation, to take advantage of favorable Coulombic interactions. This could cause anions to be “trapped” by the extensive alkyl chains, particularly when the alkyl substituents on the phosphonium cation is sufficiently large relative to the size of the anion.⁴⁴ The anions that are confined by long alkyl chains may interact more closely and strongly with the pairing cation, reducing the reactivity of the anion toward CO₂.

We recognize that an alternative interpretation of the CO₂ uptake curves would be that interaction between the cation and anion affects the *enthalpy* of the reaction between the anion and CO₂. While entirely reasonable, we currently favor the interpretation in terms of the entropy of reaction because of its consistency with the viscosity, conductivity, and “ionicity” data, as well as the CO₂ uptakes. We note that we, unfortunately, are not able to experimentally measure the enthalpy of reaction for the ILs with different cations to the accuracy that would be needed to distinguish between these two interpretations. This is because at a fixed value of $\Delta S_{\text{rxn}}^{\circ}$, a range of just 3 kJ mol⁻¹ in $\Delta H_{\text{rxn}}^{\circ}$ would be needed to explain the variation in CO₂ uptake shown in Figure 6.

CONCLUSION

In an attempt to develop ILs with both high CO₂ solubility and low viscosity, and in order to examine the effect of the cation size on physical properties and CO₂ solubilities, a series of tetraalkylphosphonium 2-cyanopyrrolide ([P_{*n*}][2-CNPy]) ILs were synthesized and characterized. This work shows that the physical properties of [P_{*n*}][2-CNPy] ILs can be readily tuned by adjusting the size of the hydrocarbon substituents on the cation. Especially, the viscosity was reduced significantly by pairing the [2-CNPy]⁻ anion with a smaller tetraalkylphosphonium cation (viscosity at room temperature decreases by 5-fold when [P₄₄₄₁₈]⁺ was replaced with [P₂₂₂₂]⁺). The [P_{*n*}][2-CNPy] ILs with a larger phosphonium cation showed a relatively low degree of ionicity compared to those with smaller cation due to strong van der Waals interactions that lead to ion pairing or formation of aggregates. Higher CO₂ solubilities were

exhibited by ILs with smaller cations, and we attribute this to a smaller entropy change for the reaction, which is related to the higher ionicity (less association and aggregation, as well as shorter interaction times) of the ILs with smaller cations. This suggests that the choice of cation has a nontrivial effect on the CO₂ solubility in addition to being primarily responsible for the physical properties. While the anion is still primarily affiliated with the CO₂ binding reaction, it was possible to achieve significantly lower viscosity and remarkably higher CO₂ solubility in gravimetric ratio simply by reducing the size of the cation, and this offers great potential for CO₂ separation using ILs.

ASSOCIATED CONTENT

Supporting Information

The Supporting Information is available free of charge on the ACS Publications website at DOI: 10.1021/acs.jpcc.5b05733.

Details on the NMR characterization for each IL synthesized; density, viscosity, conductivity, CO₂ solubility, and molar volume data in tabular form. (PDF)

AUTHOR INFORMATION

Corresponding Author

*Tel: (574) 631-5847. Fax: (574) 631-8366. E-mail: jfb@nd.edu.

Notes

The authors declare no competing financial interest.

ACKNOWLEDGMENTS

This material is based upon work supported by the Department of Energy under Award Number DE-FC26-07NT43091 (National Energy Technology Laboratory) and AR0000094 (Advanced Research Projects Agency–Energy). We thank Megan Thedwall for density measurements.

REFERENCES

- Brennecke, J. F.; Gurkan, B. E. Ionic Liquids for CO₂ Capture and Emission Reduction. *J. Phys. Chem. Lett.* **2010**, *1*, 3459–3464.
- Gurkan, B. E.; de la Fuente, J. C.; Mindrup, E. M.; Ficke, L. E.; Goodrich, B. F.; Price, E. A.; Schneider, W. F.; Brennecke, J. F. Equimolar CO₂ Absorption by Anion-Functionalized Ionic Liquids. *J. Am. Chem. Soc.* **2010**, *132*, 2116–2117.
- Goodrich, B. F.; de la Fuente, J. C.; Gurkan, B. E.; Zadigian, D. J.; Price, E. A.; Huang, Y.; Brennecke, J. F. Experimental Measurements of Amine-Functionalized Anion-Tethered Ionic Liquids with Carbon Dioxide. *Ind. Eng. Chem. Res.* **2011**, *50*, 111–118.
- Seo, S.; Quiroz-Guzman, M.; DeSilva, M. A.; Lee, T. B.; Huang, Y.; Goodrich, B. F.; Schneider, W. F.; Brennecke, J. F. Chemically Tunable Ionic Liquids with Aprotic Heterocyclic Anion (AHA) for CO₂ Capture. *J. Phys. Chem. B* **2014**, *118*, 5740–5751.
- Wang, C.; Luo, X.; Luo, H.; Jiang, D.-E.; Li, H.; Dai, S. Tuning the Basicity of Ionic Liquids for Equimolar CO₂ Capture. *Angew. Chem., Int. Ed.* **2011**, *50*, 4918–4922.
- Wang, C.; Luo, H.; Li, H.; Zhu, X.; Yu, B.; Dai, S. Tuning the Physicochemical Properties of Diverse Phenolic Ionic Liquids for Equimolar CO₂ Capture by the Substituent on the Anion. *Chem. - Eur. J.* **2012**, *18*, 2153–2160.
- Bates, E. D.; Mayton, R. D.; Ntai, I.; Davis, J. H. CO₂ Capture by a Task-Specific Ionic Liquid. *J. Am. Chem. Soc.* **2002**, *124*, 926–927.
- Zhang, Y.; Zhang, S.; Lu, X.; Zhou, Q.; Fan, W.; Zhang, X. Dual Amino-Functionalised Phosphonium Ionic Liquids for CO₂ Capture. *Chem. - Eur. J.* **2009**, *15*, 3003–3011.
- Gutowski, K. E.; Maginn, E. J. Amine-Functionalized Task-Specific Ionic Liquids: a Mechanistic Explanation for the Dramatic

Increase in Viscosity Upon Complexation with CO₂ From Molecular Simulation. *J. Am. Chem. Soc.* **2008**, *130*, 14690–14704.

(10) Gurkan, B.; Goodrich, B. F.; Mindrup, E. M.; Ficke, L. E.; Massel, M.; Seo, S.; Senftle, T. P.; Wu, H.; Glaser, M. F.; Shah, J. K.; et al. Molecular Design of High Capacity, Low Viscosity, Chemically Tunable Ionic Liquids for CO₂ Capture. *J. Phys. Chem. Lett.* **2010**, *1*, 3494–3499.

(11) Wu, H.; Shah, J. K.; Tenney, C. M.; Rosch, T. W.; Maginn, E. J. Structure and Dynamics of Neat and CO₂-Reacted Ionic Liquid Tetrabutylphosphonium 2-Cyanopyrrolide. *Ind. Eng. Chem. Res.* **2011**, *50*, 8983–8993.

(12) Xie, W.; Xie, R.; Pan, W.-P.; Hunter, D.; Koene, B.; Tan, L.-S.; Vaia, R. Thermal Stability of Quaternary Phosphonium Modified Montmorillonites. *Chem. Mater.* **2002**, *14*, 4837–4845.

(13) Wooster, T. J.; Johanson, K. M.; Fraser, K. J.; MacFarlane, D. R.; Scott, J. L. Thermal Degradation of Cyano Containing Ionic Liquids. *Green Chem.* **2006**, *8*, 691–696.

(14) Cassity, C. G.; Mirjafari, A.; Mobarrez, N.; Strickland, K. J.; O'Brien, R. A.; Davis, J. H. Ionic Liquids of Superior Thermal Stability. *Chem. Commun.* **2013**, *49*, 7590–7592.

(15) Bradaric, C. J.; Downard, A.; Kennedy, C.; Robertson, A. J.; Zhou, Y. Industrial Preparation of Phosphonium Ionic Liquids. *Green Chem.* **2003**, *5*, 143–152.

(16) Seo, S.; Simoni, L. D.; Ma, M.; DeSilva, M. A.; Huang, Y.; Stadtherr, M. A.; Brennecke, J. F. Phase-Change Ionic Liquids for Postcombustion CO₂ Capture. *Energy Fuels* **2014**, *28*, 5968–5977.

(17) Eisinger, R. S.; Keller, G. E., II. Process for CO₂ Capture Using Ionic Liquid That Exhibits Phase Change. *Energy Fuels* **2014**, *28*, 7070–7078.

(18) Gurkan, B. E.; Gohndrone, T. R.; McCready, M. J.; Brennecke, J. F. Reaction Kinetics of CO₂ Absorption in to Phosphonium Based Anion-Functionalized Ionic Liquids. *Phys. Chem. Chem. Phys.* **2013**, *15*, 7796–7811.

(19) Brown, P.; Gurkan, B. E.; Hatton, T. A. Enhanced Gravimetric CO₂ Capacity and Viscosity for Ionic Liquids with Cyanopyrrolide Anion. *AIChE J.* **2015**, *61*, 2280–2285.

(20) Xu, W.; Cooper, E. I.; Angell, C. A. Ionic Liquids: Ion Mobilities, Glass Temperatures, and Fragilities. *J. Phys. Chem. B* **2003**, *107*, 6170–6178.

(21) Yee, P.; Shah, J. K.; Maginn, E. J. State of Hydrophobic and Hydrophilic Ionic Liquids in Aqueous Solutions: Are the Ions Fully Dissociated? *J. Phys. Chem. B* **2013**, *117*, 12556–12566.

(22) MacFarlane, D. R.; Forsyth, M.; Izgorodina, E. I.; Abbott, A. P.; Annat, G.; Fraser, K. On the Concept of Ionicity in Ionic Liquids. *Phys. Chem. Chem. Phys.* **2009**, *11*, 4962–4967.

(23) Xu, D.; Yang, Q.; Su, B.; Bao, Z.; Ren, Q.; Xing, H. Enhancing the Basicity of Ionic Liquids by Tuning the Cation–Anion Interaction Strength and via the Anion-Tethered Strategy. *J. Phys. Chem. B* **2014**, *118*, 1071–1079.

(24) Hollóczki, O.; Kelemen, Z.; Könczöl, L.; Szieberth, D.; Nyulászi, L.; Stark, A.; Kirchner, B. Significant Cation Effects in Carbon Dioxide-Ionic Liquid Systems. *ChemPhysChem* **2013**, *14*, 315–320.

(25) Rodríguez, H.; Gurau, G.; Holbrey, J. D.; Rogers, R. D. Reaction of Elemental Chalcogens with Imidazolium Acetates to Yield Imidazole-2-Chalcogenones: Direct Evidence for Ionic Liquids as Proto-Carbenes. *Chem. Commun.* **2011**, *47*, 3222–3224.

(26) Gurau, G.; Rodríguez, H.; Kelley, S. P.; Janiczek, P.; Kalb, R. S.; Rogers, R. D. Demonstration of Chemisorption of Carbon Dioxide in 1,3-Dialkylimidazolium Acetate Ionic Liquids. *Angew. Chem., Int. Ed.* **2011**, *50*, 12024–12026.

(27) Shiflett, M. B.; Elliott, B. A.; Lustig, S. R.; Sabesan, S.; Kelkar, M. S.; Yokozeki, A. Phase Behavior of CO₂ In Room-Temperature Ionic Liquid 1-Ethyl-3-Ethylimidazolium Acetate. *ChemPhysChem* **2012**, *13*, 1806–1817.

(28) Cabaço, M. I.; Besnard, M.; Danten, Y.; Coutinho, J. A. P. Carbon Dioxide in 1-Butyl-3-Methylimidazolium Acetate. I. Unusual Solubility Investigated by Raman Spectroscopy and DFT Calculations. *J. Phys. Chem. A* **2012**, *116*, 1605–1620.

(29) Besnard, M.; Cabaço, M. I.; Chávez, F. V.; Pinaud, N. On the Spontaneous Carboxylation of 1-Butyl-3-Methylimidazolium Acetate by Carbon Dioxide. *Chem. Commun.* **2012**, *48*, 1245–1247.

(30) Seo, S.; DeSilva, M. A.; Brennecke, J. F. Physical Properties and CO₂ Reaction Pathway of 1-Ethyl-3-Methylimidazolium Ionic Liquids with Aprotic Heterocyclic Anions. *J. Phys. Chem. B* **2014**, *118*, 14870–14879.

(31) Gohndrone, T. R.; Lee, B. T.; DeSilva, M. A.; Quiroz-Guzman, M.; Schneider, W. F.; Brennecke, J. F. Competing Reactions of CO₂ With Cations and Anions in Azolide Ionic Liquids. *ChemSusChem* **2014**, *7*, 1970–1975.

(32) Hamilton, P. A.; Murrells, T. P. Kinetics and Mechanism of the Reactions of PH₃ With O(³P) and N(⁴S) Atoms. *J. Chem. Soc., Faraday Trans. 2* **1985**, *81*, 1531–1541.

(33) Lee, B. I.; Kesler, M. G. A Generalized Thermodynamic Correlation Based on Three-Parameter Corresponding States. *AIChE J.* **1975**, *21*, 510–527.

(34) Tokuda, H.; Hayamizu, K.; Ishii, K.; Susan, M.; Watanabe, M. Physicochemical Properties and Structures of Room Temperature Ionic Liquids. 2. Variation of Alkyl Chain Length in Imidazolium Cation. *J. Phys. Chem. B* **2005**, *109*, 6103–6110.

(35) Yoshii, K.; Yamaji, K.; Tsuda, T.; Tsunashima, K.; Yoshida, H.; Ozaki, M.; Kuwabata, S. Physicochemical Properties of Tri-N-Butylalkylphosphonium Cation-Based Room-Temperature Ionic Liquids. *J. Phys. Chem. B* **2013**, *117*, 15051–15059.

(36) Fredlake, C. P.; Crosthwaite, J. M.; Hert, D. G.; Aki, S. N. V. K.; Brennecke, J. F. Thermophysical Properties of Imidazolium-Based Ionic Liquids. *J. Chem. Eng. Data* **2004**, *49*, 954–964.

(37) Fang, D. W.; Guan, W.; Tong, J.; Wang, Z. W.; Yang, J. Z. Study on Physicochemical Properties of Ionic Liquids Based on Alanine [C_nmim][Ala] (n = 2,3,4,5,6). *J. Phys. Chem. B* **2008**, *112*, 7499–7505.

(38) Tariq, M.; Forte, P. A. S.; Gomes, M. F. C.; Lopes, J. N. C.; Rebelo, L. P. N. Densities and Refractive Indices of Imidazolium- and Phosphonium-Based Ionic Liquids: Effect of Temperature, Alkyl Chain Length, and Anion. *J. Chem. Thermodyn.* **2009**, *41*, 790–796.

(39) Kagimoto, J.; Taguchi, S.; Fukumoto, K.; Ohno, H. Hydrophobic and Low-Density Amino Acid Ionic Liquids. *J. Mol. Liq.* **2010**, *153*, 133–138.

(40) Shannon, M. S.; Bara, J. E. Properties of Alkylimidazoles as Solvents for CO₂ Capture and Comparisons to Imidazolium-Based Ionic Liquids. *Ind. Eng. Chem. Res.* **2011**, *50*, 8665–8677.

(41) Tsunashima, K.; Kawabata, A.; Matsumiya, M. Low Viscous and Highly Conductive Phosphonium Ionic Liquids Based on Bis-(Fluorosulfonyl)Amide Anion as Potential Electrolytes. *Electrochem. Commun.* **2011**, *13*, 178–181.

(42) Vogel, H. The Temperature Dependence Law of the Viscosity of Fluids. *Phys. Z.* **1921**, *22*, 645–646.

(43) Ueno, K.; Tokuda, H.; Watanabe, M. Ionicity in Ionic Liquids: Correlation with Ionic Structure and Physicochemical Properties. *Phys. Chem. Chem. Phys.* **2010**, *12*, 1649–1658.

(44) Fraser, K. J.; Izgorodina, E. I.; Forsyth, M.; Scott, J. L.; MacFarlane, D. R. Liquids Intermediate Between “Molecular” and “Ionic” Liquids: Liquid Ion Pairs? *Chem. Commun.* **2007**, *0*, 3817–3819.

(45) Aki, S. N. V. K.; Mellein, B. R.; Saurer, E. M.; Brennecke, J. F. High-Pressure Phase Behavior of Carbon Dioxide with Imidazolium-Based Ionic Liquids. *J. Phys. Chem. B* **2004**, *108*, 20355–20365.

(46) Shariati, A.; Peters, C. J. High-Pressure Phase Behavior of Systems with Ionic Liquids: II. the Binary System Carbon Dioxide+1-Ethyl-3-Methylimidazolium Hexafluorophosphate. *J. Supercrit. Fluids* **2004**, *29*, 43–48.

(47) Yunus, N. M.; Mutalib, M. I. A.; Man, Z.; Bustam, M. A.; Murugesan, T. Solubility of CO₂ in Pyridinium Based Ionic Liquids. *Chem. Eng. J.* **2012**, *189*, 94–100.

(48) Goodrich, B. F.; de la Fuente, J. C.; Gurkan, B. E.; Lopez, Z. K.; Price, E. A.; Huang, Y.; Brennecke, J. F. Effect of Water and Temperature on Absorption of CO₂ By Amine-Functionalized Anion-Tethered Ionic Liquids. *J. Phys. Chem. B* **2011**, *115*, 9140–9150.